ARTICLE NO. 79-4067

Identification of a STOL Propulsion Plant Model from Flight Data

Ronald L. De Hoff*
Systems Control, Inc. (Vt), Palo Alto, Calif.

Accurate dynamic models for propulsion system behavior are critical to successful synthesis of STOL autothrottle/autoland control systems. This paper describes the development of a nonlinear dynamic model for the response of a STOL aircraft in the landing/approach configuration. The model is based upon an analysis of the throttle, governor, and turbofan engine components. Model parameters are directly identified from data acquired during a flight of the NASA Augmentor Wing Jet STOL research aircraft. The accuracy of the model and a comparison of results for two engines are described. Various approaches to modeling propulsion system response for complex systems representative of current and near-term aircraft are discussed.

Nomenclature

a_0 = throttle hysteresis proportional to throttle level
a_1 = throttle hysteresis independent of throttle level
b_0 = throttle pickoff bias
b_1 = throttle pickoff scale factor
C_{FB} = pressure drop governor positive feedback
C_{FH} = fuel flow to compressor speed coupling coefficient
C_{HL} = high spool to low spool coupling coefficient
d_1 = hysteresis exterior to governor
d_2 = internal governor hysteresis
f = nonlinear engine dynamics function vector
g_1, g_2, g_3 = governor control parameters
h = nonlinear measurement distribution function vector
i = time index subscript
J = estimation likelihood function
k = time subscript
K_{AF} = orifice area to fuel flow conversion factor
K_{DL} = low rotor to duct pressure coupling coefficient
K_{EH} = engine speed to tailpipe pressure coupling coefficient
K_p = proportional governor gain
K_{SF} = fuel flowmeter scale factor
K_{TH} = throttle deflection to speed command conversion factor
$\dot{m}_a$ = engine airflow
N = number of data points
N_H = compressor speed
N_{HM} = measured compressor speed
N_{HO} = compressor speed equilibrium offset
N_L = fan speed
N_{LM} = measured fan speed
N_{LO} = fan speed equilibrium offset
p = number of measurements
P_D = duct pressure
P_{DM} = measured duct pressure
P_{DO} = duct pressure equilibrium offset
P_T = tailpipe pressure
P_{TM} = measured tailpipe pressure
P_{TO} = tailpipe pressure equilibrium offset
R = covariance matrix for sensor noise
T_H = engine thrust due to engine exhaust
T_C = engine thrust due to ducted/fan airflow
u = control vector
v_k = random instrument noise process
W_F = fuel flow
W_{FE} = estimated fuel flow
W_{FM} = measured fuel flow
W_{FO} = fuel flow equilibrium offset
x = state vector
y = measurement vector
α = fuel flow-compressor speed coupling ratio
Γ = discrete control distribution matrix
δ = deflection variable
δ_c = commanded deflection
δ_T = throttle deflection
δ_{TM} = measured throttle deflection
ζ = flow meter damping ratio
ϵ = governor speed error
θ = model parameter vector
μ = quadratic governor orifice characteristic parameter
Φ = state transition matrix
σ = standard deviation of measurement noise
τ_D = duct pressure time constant
τ_E = tailpipe pressure time constant
τ_H = collective speed time constant
τ_L = differential speed time constant
ω = natural frequency (undamped) of flowmeter
$\hat{(\ )}$ = estimated value
$\dot{(\ )}$ = derivative with respect to time
$(\ )^T$ = matrix transpose

Received April 7, 1978; revision received July 5, 1978.

Index categories: Airbreathing Propulsion; Simulation; Testing, Flight and Ground.

*Senior Engineer, System Identification and Control Division. Member AIAA.

I. Introduction

PROPOSED propulsion system designs for V/STOL aircraft differ radically from modern aircraft turbomachine configurations. Reliability, controlability, and overall performance requirements have dictated complex interconnections and distribution of propulsion components throughout the airframe. The modeling of the dynamic response of such systems in their installed environment is quickly becoming a critical consideration in the design and evaluation of integrated flight controls for such aircraft. Simplified techniques which do not consider physical interactions tend to yield inconsistent and unacceptable results when used as synthesis or evaluation tools for control design.

The Augmentor Wing Jet STOL Research Aircraft, maintained by NASA Ames Research Center, is an advanced testbed for STOL flight testing. Vehicle control is important when closely tracking an altitude profile during approach and

flare maneuvers. For a powered-lift vehicle during landing approach, the throttle may be used as the primary control of normal acceleration. The accurate digital simulation of aircraft maneuvers involving throttle changes and the design of autopilot logic using feedback to the throttle require an accurate model of the dynamic response of engine thrust to changes in throttle commands.

The aircraft is a modified de Havilland Buffalo C8-A aircraft using two Rolls Royce Spey engines.[1] Modifications to the aircraft were made to improve lift characteristics at low speed for the short landing requirement. A transverse duct is used to channel a portion of the fan airflow to ejector nozzles on the opposite wing blowing over an augmentor flap. Direct lift is provided by vectoring core stream flow through an adjustable nozzle. The modifications cause a significant dynamical coupling between the engines and aircraft. An accurate engine model, verified from flight data, is desirable to simulate these effects.

The Spey engine is a low-bypass twin-spool turbofan. The normal gas path has been significantly modified for STOL operation. The new configuration is shown in Fig. 1. The engine fuel control is hydromechanical. A cable linkage connects throttle lever inputs from the cockpit electromechanical servo to the engine.

Several approaches to propulsion system modeling are described in Sect. II. In Sec. III, the development of the form of the engine model is described along with a description of the initial parameter estimates. Section IV describes the parameter estimation procedure and the results from the parameter identification process. Conclusions concerning the accuracy of the technique and the general applicability are presented in Sec. V.

II. Types of Engine Models

Any propulsion system can be described in mathematical terms in several ways. The choice of model form has an important impact on the analysis tools, the sensor requirements and the regimes of application of the equations. Another consideration is the interface between the system and the input/output boundaries. Models that describe the throttle linkage and fuel control as well as the engine may be significantly different from those considering the engine alone.

In this case, a model is desired which describes the engine thrust and airflow response to power lever inputs from the cockpit.[2] Small throttle perturbation response near high power must be accurately represented. The model will be used to approximately describe large power excursions. Low altitude and speed conditions represent the important flight regime.

The model will be used to predict engine performance. Steady-state thrust and airflow should match static tests corrected to nonstandard conditions. Dynamic response to small perturbations should accurately reflect engine behavior. Match of internal variables describing engine operation is not critical.

Models used to describe typical engine behavior vary widely in complexity and accuracy.[3-5] The simplest description of engine response is to plot corrected engine thrust vs power lever angle. This characteristic is shown in Fig. 2. The plot can be used as a dynamic model if an appropriate time lag is associated between the actual throttle position and a virtual position. The engine is observed to accelerate and decelerate at rates dependent on the power level. This effect can be represented as a variable rate limit as shown in Fig. 3. No attempt is made at a phenomenological explanation of the behavior, and parameters are adjusted from observations. Since the model does not reflect the internal derivative agents of thrust response, the match between the system behavior for various size inputs and for different starting and ending points is problematic. A more significant aspect is the possibly poor *closed-loop* description of the response. This is manifested by an inaccurate prediction of closed-loop stability, a fact primarily due to matching step response rather than to frequency response over a suitable range. In order to accommodate this lack of precision, simple models tend to be "improved" by ad hoc additions which attempt to correct the fundamental nonphenomenological characteristics of the formulation.

Far more complex digital simulations exist which include engine component characteristics measured from rig tests and aerothermodynamic phenomena occuring in the gas path.[5] These simulations apply basic physical laws relating energy, work, massflow, and acceleration. Various "adjustable" parameters, such as lumped isentropic efficiencies and areas, are manipulated to match the observed steady-state relationship between input and output variables. The overall response can be generally tuned to mimic observed dynamics. This type of simulation recreates steady-state performance accuracy. Transient response matches may suffer due to parameter uncertainties in the complex equations. Predicted stability characteristics in a closed-loop control are quite good.

The drawbacks of detailed analytical simulations are that: 1) a large computer capability is necessary to execute them (often slower than real time); 2) detailed internal engine and control information is required which is only available, if at all, to the engine manufacturer; and 3) the added complexity cannot be justified or validated from input/output performance observed in operation. Clearly, a middle ground must exist.

The development of an experimentally validated analytical description of the propulsion system can be accomplished by

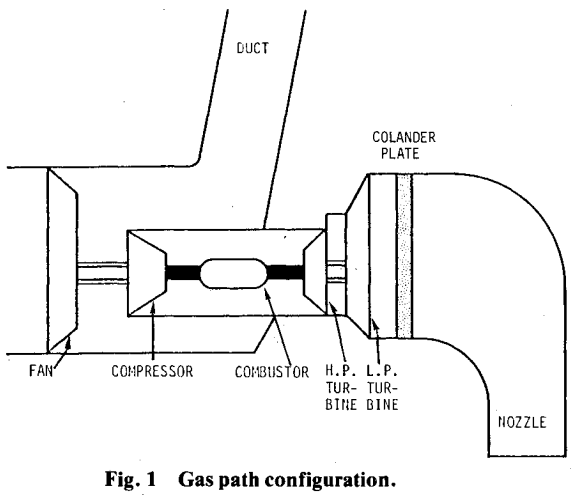

Fig. 1 Gas path configuration.

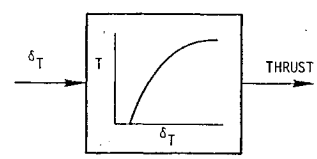

Fig. 2 Thrust response to throttle input.

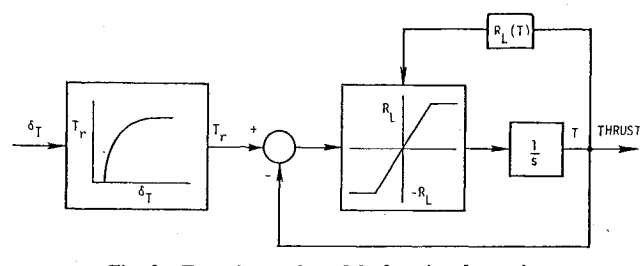

Fig. 3 Experimental model of engine dynamics.

considering the available measurement data and the type of inputs provided. The development starts with an analysis of possible dynamic effects. Data are examined and unimportant or unexcited phenomena are removed. Several analytical procedures exist to assist in making this determination and validating the model structure:[6] The remaining model terms are examined for bandwidth of response relative to the simulation requirement. High-frequency effects can be neglected. The resulting system represents the response including both steady-state and dynamic performance whose parameterization is available from recorded measurements. This type of model can be used in an overall aircraft simulation for the validation of outer-loop integrated control functions such as flight direction and autothrottle.

III. Development of Spey Engine Model

The Spey engine is characterized by a group of nonlinear dynamical elements: 1) the engine, 2) the fuel control, and 3) the throttle linkage. Models can be derived for the physical members of the system. These can be simplified to contain only those elements which can be estimated from the flight data.

The dynamics of the engine in the region near full power are nearly linear. Small perturbations in the engine are characterized by the rotor speed response. Previous analysis[3] of turbofan dynamics has verified the model linearity and the structure using techniques describe in Ref. 6.

The engine behavior during moderate speed excursions can be simplified to second order. The response is the sum of *collective* rotor speed variations and *differential* speed changes between the spools. For example, pertubations in fuel flow cause the two engine spools to accelerate in a collective fashion. Perturbations in fan loading due to variations in duct pressure or inlet distortion cause the fan and compressor speeds to differentially rematch.

The linear system is shown in state variable form as follows:

$$\begin{bmatrix}\delta\dot{N}_L\\ \delta\dot{N}_H\end{bmatrix}=\begin{bmatrix}-1/\tau_L & C_{HL}(1-\alpha)\\ 0 & -1/\tau_H\end{bmatrix}\begin{bmatrix}\delta N_L\\ \delta N_H\end{bmatrix}+\begin{bmatrix}\alpha C_{FH}C_{HL}\\ C_{FH}\end{bmatrix}\delta W_f \tag{1}$$

where the five linear parameters τ_L, τ_H, C_{HL}, C_{FH} and α model the behavior of the engine.

The dynamical equations are written for perturbations away from an equilibrium condition. A typical choice for this equilibrium point is 100% power.

The flow equation for the pressures in the duct and nozzle can be linearized as follows:

$$\delta\dot{p}_D=-(\delta P_D-K_{DL}\delta N_L)/\tau_D \tag{2a}$$

Table 1 Sensor list

Variable	Symbol	Sensor white noise level, [a] %
Low rotor speed	N_L	0.5
High rotor speed	N_H	0.5
Throttle command	δ_c	1.0
Throttle angle	δ_T	1.0
Duct pressure	P_D	2.0
Exhaust pressure	P_E	2.0
Fuel flow	W_F	2.0

[a] Standard deviation as percent of full scale.

$$\delta\dot{p}_E=-(\delta p_E-K_{EH}\delta N_H)/\tau_E \tag{2b}$$

where temperature dependence is ignored, and the mass flows are modeled as linear functions of the perturbational rotor speeds which feed the duct and exhaust volumes. It is expected that the flow time constants will be small compared to the rotor lags.

Engine power requests from the cockpit are transferred by a mechanical linkage driven by an electromechanical force servo. The system contains a moderate amount of hysteresis which affects small inputs typical of autothrottle landing commands.

The speed governor, which regulates fuel metering, can be approximated by the following control law[2]:

$$W_f=K_p(g_1+g_2X_c-g_3N_H^2)N_H \tag{3}$$

where X_c is the throttle command, W_f is the fuel flow, and N_H is the compressor speed. For large power transients, metering area saturation removes the last term in Eq. (3) and the control law is unstable; i.e., increased speed increases the fuel.

The system model can be simplified to include the linear model of the engine, a hysteresis model of the throttle linkage, and a model of the hydromechanical governor (see Fig. 4).

Data on Spey performance was acquired in flight. Instrumentation was used as listed in Table 1. Speed, position, and pressure transducers responded faster than the dynamics being estimated. The measurement errors associated with these inputs can be considered uncorrelated random processes with rms values shown in the table.

The instrument noise was estimated from the data records by calculating the sample variance from steady-state portions of the flight. The noise was verified to be nearly white and uncorrelated between channels. These figures are used to form the sensor error variance matrix R discussed in Sec. IV.

The fuel flow sensor was a restrained turbine whose angular deflection was proportional to the turbine torque and mass flow. The meter's response was lightly damped because of the small damping supplied by the turbine. A flowmeter model was developed and included in the simulation.

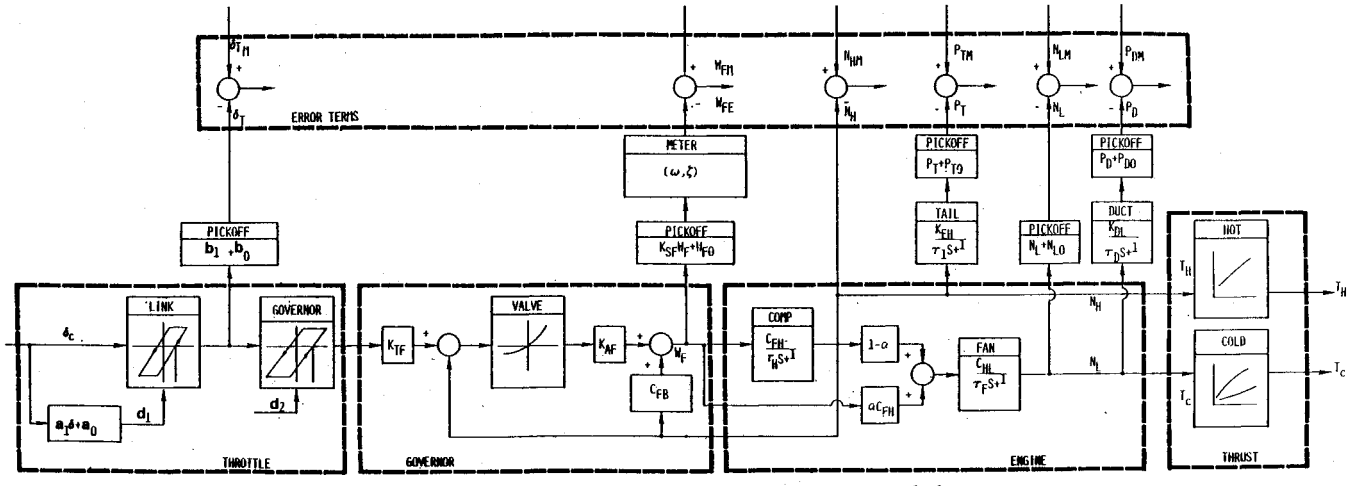

Fig. 4 Spey engine identification model showing program symbology.

Table 2 Engine state, output, and control vectors

State vector (x)
High rotor speed
Low rotor speed
Tailpipe pressure
Duct pressure
Control vector (u)
Throttle position
Measurement vector (y)
Throttle pickoff
Fuel flow
High rotor speed
Low rotor speed
Tailpipe pressure
Duct pressure

Flight data were taken in the approach configuration in a powered descent from 7500 ft. The nozzles in this configuration are rotated downward and the engines are operating near full power. The flight computer was used to generate throttle rate commands to the electromechanical servo. The engine throttles were modulated in unison.

IV. Parameter Estimation Results

The Spey engine model discussed in Sec. III is used as the foundation of the parameter estimation procedure. The model equations can be represented as follows:

$$\dot{x}=f(x,u,\theta) \tag{4}$$

$$y_k=h(x_k,u_k,\theta)+v_k \tag{5}$$

where the x is the engine state vector, y is the measurement vector, and f and h are the engine/control dynamic equations and measurement distribution functions, respectively. Table 2 lists the element of the state, output, and control vectors. The measurement noise is assumed to have a Gaussian distribution with known covariance (see Table 1) and it is assumed that there is no process noise.

The maximum likelihood parameter estimates are obtained by minimizing the log-likelihood function for the parameter estimate given the data.[7]

$$J=\min_{\theta}\sum_{i=1}^{N}[y(i)-\hat{y}(i)]^{T}R^{-1}[y(i)-\hat{y}(i)] \tag{6}$$

where $R=\mathrm{diag}(\sigma_1^2,\ldots,\sigma_p^2)$ is the covariance matrix of the independent measurement error and N is the number of data points.

$$\hat{y}(i)=h[\hat{x}(i),u(i),\hat{\theta}) \tag{7}$$

subject to the differential constraint

$$\dot{\hat{x}}=f(\hat{x},u,\hat{\theta}) \tag{8}$$

where $\hat{\theta}$ is the estimated value of the model parameters.

The model equations are implemented in a dynamic simulation of the engine. The parameter estimation routine executes the simulation with the inputs occurring in the data record and a trial set of model parameter variables. The cost function is calculated from the simulated and actual outputs. After the parameters are estimated, the simulation code is available for implementation in a full flight simulator program.

For the engine model Eq. (8) is discretized internally in the simulation program to form the discrete constraint equations:

$$\hat{x}(i+1)=\phi\hat{x}(i)+\Gamma u(i) \tag{9}$$

The iterative minimization in Eq. (6) can be performed using either a quasi-Newton method or Levenberg-Marquardt procedure.[8] The Levenberg-Marquardt algorithm provides a stable search for the minima near a priori estimates. The parameter step for this algorithm is as follows:

$$\hat{\theta}(i+1)=\hat{\theta}(i)-\left[\frac{\partial^2 J}{\partial\theta^2}\bigg|_{\theta=\hat{\theta}(i)}+\lambda I\right]^{-1}\frac{\partial J}{\partial\theta}\bigg|_{\theta=\hat{\theta}(i)} \tag{10}$$

where the expression

$$\frac{\partial^2 J}{\partial\theta^2}\bigg|_{\theta=\hat{\theta}(i)}$$

is approximated from gradient calculations, and the Marquardt parameter, λ, is chosen based on algorithm performance during the search.

The parameter estimation procedure described produces the maximum likelihood estimates for a given data record, assuming the correct model structure and no process disturbances.[9] The model structure has been carefully studied and initially evaluated to assure good a priori parameter estimates.[2,6] Process noise effects were not observed.

The identification procedure was used to identify parameters in portions of the engine using measured or derived variables as input. The program was sequentially exercised to identify throttle parameters, engine pressure dynamics, engine dynamics, and engine/control dynamics.

The parameter accuracy was evaluated from estimates of their standard deviation (F-ratio), from run-to-run repeatability, and from predictive capability of the outputs using nongenerating data records.

Run-to-run consistency is shown in Table 3 for three different input experiments. In this case, fuel flow was considered the input variable and the two rotor speeds and duct pressures formed the error terms. Final parameter estimates were calculated by combining single run parameter estimates weighted with the estimated dispersion. The final parameter estimates were then used to predict the engine response generated by a random sequence of throttle inputs. The results shown in Fig. 5 and indicate that the model performance is generally good in predicting steady state and transient behavior.

The final parameter values are listed in Table 4 for the left and right engine along with the estimated confidence intervals.

The hysteresis levels and throttle pickoff parameters were identified accurately and repeatably. Parameters representing the engine response varied around 10% between the left and right engine except for the collective spool time constant. Here, a significant (35%) difference was noted between engines. The domiant time constant representing the engine and governor system, varied by an equivalent amount. This may represent an effect important in evaluating autothrottle response. Differences of this type are attributed to build or deterioration and have been used as performance monitoring variables to influence overhaul and maintenance decisions.[10]

V. Summary and Conclusions

The Spey engines represent a complex system of coupled dynamics. Flight data was acquired during controlled throttle tests in the powered-lift approach configuration of the aircraft. A dynamical model of the throttle linkage, control system, engines, and duct was developed from an analysis of the physical configuration of the engine. A system identification program was used to process the flight data and estimate engine model parameters.

The quality of the flight data was excellent. Inputs controlled by the avionics computer were exceptionally repeatable, and accuracies associated with parameters were quite good for this reason. The data processing was nearly

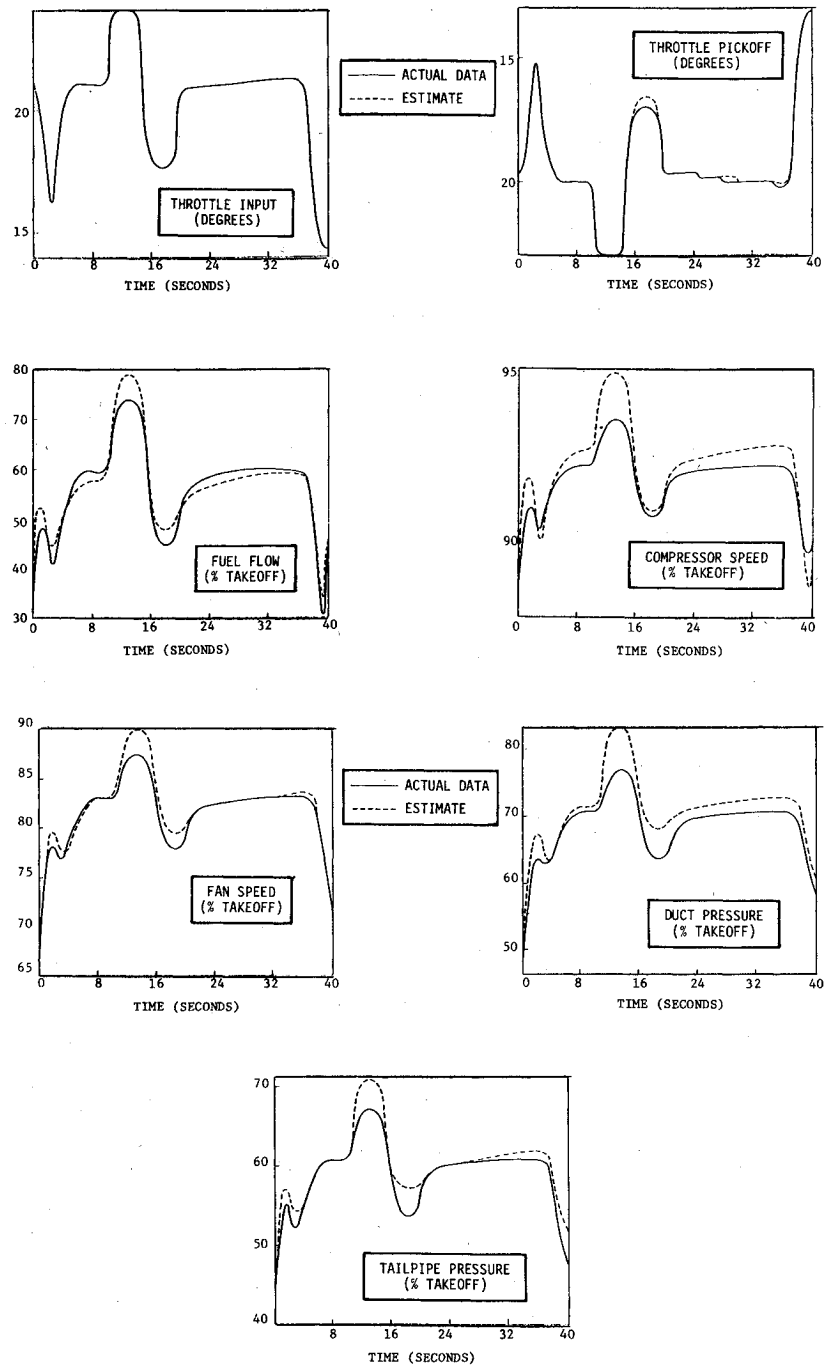

Fig. 5 Results of model verification on throttle transient response data for the Spey engine.

Table 3 Run-to-run repeatability of engine parameter estimates

	Record no. 1 – 3000 Pts		Record no. 2 – 3000 pts		Record no. 3 – 2000 pts.	
	Estimate	Std. dev.[a]	Estimate	Std. dev.[a]	Estimate	Std. dev.[a]
τ_L	0.246	1.8	0.210	1.3	0.281	1.7
C_F	0.113	0.2	0.110	0.3	0.132	0.5
α	0.606	6.5	0.710	8.3	0.648	4.7
C_{HL}	2.71	1.1	3.07	0.7	3.56	0.3
τ_F	0.396	0.8	0.403	3.5	0.472	0.6
K_{EH}	4.91	0.4	4.72	0.3	4.04	0.6
K_{DL}	1.47	1.4	1.14	0.6	1.33	0.8
P_{DO}	−3.20	5.4	−3.93	1.6	−4.59	4.2
P_{TO}	−1.75	5.3	−1.94	3.8	−8.53	2.4
N_{LO}	0.274	2.1	0.324	2.3	0.388	0.3

[a] Estimated standard deviation as percent of estimate.

Table 4 Final Spey engine parameter estimates

Parameter	Left engine		Right engine	
	Estimate	Estimated uncertainty	Estimate	Estimated uncertainty
a_0	0.252	±0.062	0.254	±0.060
a_1	[a]	[a]	[a]	[a]
b_0	982	±5.0	942	±5.0
b_1	−26.3	±0.22	−24.8	±0.18
d_2	[a]	[a]	[a]	[a]
K_{TH}	0.7212[d]	...	0.7212[d]	...
μ	0[e]	...	0[e]	...
K_{AF}	3.11	±0.07	2.96	0.07
C_{FH}	0.114[c]	±0.001	0.118[c]	±0.002
ξ	0.2[b]	±0.2[b]	0.2	±0.2
ω	13[b]	±3[b]	13[b]	±3[b]
τ_H	0.232	±0.011	0.312	±0.022
C_{FB}	0.114	±0.001	0.118	±0.002
α	0.64	±0.13	0.56	±0.10
C_{HL}	3.39	±0.07	3.02	±0.07
τ_F	0.437	±0.02	0.423	±0.02
$1/\tau_E$	0	±0.001	0	±0.001
K_{EH}	4.10	±0.10	4.35	±0.40
$1/\tau_D$	0.05	...	0.05	...
K_{DL}	1.36	±0.01	1.40	±0.3
K_{SF}	1.0[e]	...	1.0[e]	...
Wf_0	0.0[e]	...	0.0[e]	...
P_{TO}	−3.02	±0.09	−3.53	±2.75
P_{DO}	5.41	±0.5	−1.82	±2.18
N_{LO}	0.382	±0.03	0.370	±0.03
(τ_{engine})	0.65	±0.05	0.89	±0.05

[a] Not significant.
[b] Estimate from inspection.
[c] Defined as equal to CF^2.
[d] Derived from steady-state operating line.
[e] No significant estimate derived from data.

routine with the identification, and run-to-run repeatability of the parameter estimates was good.

The results indicate that the engine was represented, for outer-loop simulation and control evaluation, as a second-order system. Thrust outputs had to be scheduled on fan and compressor speeds separately to model the forces generated by the engines. The behavior of the engine and control, aside from the hysteresis, was linear. An insignificant asymmetry in the acceleration and rates was found for these power levels.

The engine-to-engine repeatability of the parameter estimates was within 10% except for the collective time constant. The right engine time constant has 35% longer than the left. Differential speed responses were the same. The fuel flow to rotor speed gains were nearly the same; hence, the engine fuel consumptions were nearly equal. Differential speed responses were 50% slower than collective time constants.

The utilization of automated parameter identification procedures has provided a significant improvement over classical methods. The number of parameters estimated is far greater than previously available from graphical techniques. Run-to-run repeatability has been demonstrated for many of the variables.

Acknowledgments

This work was sponsored by the National Aeronautics and Space Administration under Contract No. 36074-13. The technical monitor at NASA Ames Research Center was D. Watson.

References

[1] Cleveland, W.B., Vomaske, R.F., and Sinclair, S.R.M., "Augmentor Wing Jet STOL Research Aircraft Digital Simulation," NASA TM X-62 149, April 1972.

[2] DeHoff, R.L., Trankle, T.L., Reed, W.B., "Identification of Spey Engine Dynamics in the Augmentor Wing STOL Research Aircraft from Flight Data," NASA CR-152054, Oct. 1977.

[3] DeHoff, R.L. and Hall, Jr., W.E., "System Identification Principles Applied to Multivariable Control and Performance Monitoring of the F100 Engine," presented at 1977 JACC, San Francisco, Calif., July 1977.

[4] DeHoff, R.L., and Hall, Jr., W.E., "Multivariable Quadratic Synthesis of an Advanced Turbofan Engine Controllers," *Journal of Guidance and Control,* Vol. 1, March-April 1978, p. 136 ff.

[5] Szuch, J. and Seldner, K, "Real Time Simulation of the F100-PW-100 Turbofan Engine Using the Hybrid Computer," NASA TM X-3261, Aug. 1975.

[6] Gupta, N.K., Hall, Jr., W.E., and Trankle, T.L., "Advanced Methods of Model Structure Determination from Test Data," *Journal of Guidance and Control,* Vol. 1, May-June 1978, p. 187 ff.

[7] Hall, Jr., W.E., Gupta, N.K., and Smith, R.G., "Identification of Aircraft Stability and Control Coefficients for the High Angle-of-Attack Regime," Technical Report No. 2, prepared for Office of Naval Research under Contract N00014-72-C-0328, March 1974.

[8] Marquardt, D.W., "An Algorithm for Least Squares Estimation of Nonlinear Parameters," *Journal of the Society of Industrial Applied Mathematics,* Vol. 11, June 1963, p. 431 ff.

[9] Gupta, N.K. and Mehra, R.K., "Computational Aspects of Maximum Likelihood Estimation and Reduction in Sensitivity Function Calculations," *IEEE Transactions on Automatic Control,* Vol. AC-19, Dec. 1974, p. 774 ff.

[10] Caspi, P., Rault, A., and Esmenjaud, O., "Etude D'un Systeme de Maintenance Preventive Personnalisee par Diagnostic et Pronostic de Dannes," AGARD -CP-165, Liege, Belgium, April 1974, p. 8-1 ff.